

# Pre-treatment effect on the structure of bacterial cellulose from Nata de Coco (*Acetobacter xylinum*)

Rusaini Athirah Ahmad Rusdi<sup>1)</sup>, Norhana Abdul Halim<sup>1), \*)</sup> (ORCID ID: 0000-0001-8077-824X), Mohd Nurazzi Norizan<sup>1)</sup> (0000-0001-7697-0511), Zul Hazrin Zainal Abidin<sup>2)</sup>, Norli Abdullah<sup>1)</sup> (0000-0002-8519-3379), Fadhlina Che Ros<sup>1)</sup>, Nurazlin Ahmad<sup>1)</sup> (0000-0002-3119-2653), Ahmad Farid Mohd Azmi<sup>1)</sup>

DOI: [dx.doi.org/10.14314/polimery.2022.3.3](https://dx.doi.org/10.14314/polimery.2022.3.3)

**Abstract:** This paper presents a structural analysis of various methods to produce bacterial cellulose (BC) from Nata de Coco (*Acetobacter xylinum*). BC sheet, BC chem and BC mech powders were successfully prepared using oven drying, chemical and mechanical treatment. The X-ray diffraction (XRD), Fourier transform infrared (FTIR) spectroscopy, and field emission scanning electron microscopy (FESEM) were used to analyze the structure of prepared BC. The structure of bacterial cellulose was compared with the structure of commercial microcrystalline cellulose (MCC) and cotton fabric. The XRD results showed that the BC sheet sample had the highest degree of crystallinity (81.76%) compared to cotton cellulose (75.73%). The crystallite size of cotton was larger than the BC sheet, with the value of 6.83 nm and 4.55 nm, respectively. The peaks in the FTIR spectra of all BC were comparable to the commercial MCC and cotton fabrics. FESEM images showed that the prepared BC sheet, BC mech, and BC chem had an almost similar structure like commercial MCC and cotton fabric. It was concluded that simple preparation of BC could be implemented and used for further BC preparation as reinforcement in polymer composites, especially in food packaging.

**Keywords:** bacterial cellulose, structure, X-ray diffraction, Fourier transform infrared spectroscopy, field emission scanning electron microscopy.

## Wpływ wstępnej obróbki na strukturę celulozy bakteryjnej z Nata de Coco (*Acetobacter xylinum*)

**Streszczenie:** Niniejszy artykuł zawiera analizę struktury celulozy bakteryjnej (BC) wytworzonej z Nata de Coco (*Acetobacter xylinum*) różnymi metodami. Folia BC i proszki BC chem oraz BC mech zostały wytworzone poprzez suszenie w piecu, obróbkę chemiczną i mechaniczną. Do oceny struktury celulozy bakteryjnej stosowano dyfrakcję rentgenowską (XRD), spektroskopię Fouriera w podczerwieni (FTIR) i skaningową mikroskopię elektronową z emisją polową (FESEM). Strukturę celulozy bakteryjnej porównano ze strukturą handlowej celulozy mikrokrystalicznej (MCC) i tkaniny bawełnianej. Wyniki XRD wykazały, że najwyższy stopień krystaliczności miała próbka arkusza BC (81,76%) w porównaniu z celulozą bawełnianą (75,73%). Wielkość kryształitów bawełny była większa niż folii BC i wynosiła, odpowiednio, 6,83 nm oraz 4,55 nm. Piki widm FTIR wszystkich otrzymanych form celulozy bakteryjnej były porównywalne z komercyjnymi tkaninami bawełnianymi i z celulozą mikrokrystalicznej. Zdjęcia FESEM folii BC oraz proszków BC mech i BC chem również były podobne do komercyjnej MCC i tkaniny bawełnianej. Stwierdzono, że z wykorzystaniem prostych technik można otrzymać BC, która może być stosowana jako wzmocnienie w kompozytach polimerowych, w szczególności w opakowaniach do żywności.

**Słowa kluczowe:** celuloza bakteryjna, struktura, dyfrakcja rentgenowska, spektroskopia w podczerwieni z transformacją Fouriera, skaningowa mikroskopia elektronowa z emisją polową.

Cellulose, which is the main component of plant cell walls like kenaf fiber [1, 2], sugar palm fiber [3, 4], bamboo [5, 6], and oil palm empty fruit bunch (OPEFB) fiber [7, 8], is the most abundant natural polymer on

<sup>1)</sup> Centre for Defence Foundation Studies, National Defence University of Malaysia, Kem Sungai Besi, 57000 Kuala Lumpur, Malaysia.

<sup>2)</sup> Centre for Ionics University Malaya (C.I.U.M), Department of Physics, Faculty of Science, University Malaya, 50603 Kuala Lumpur, Malaysia

\*) Author for correspondence: [norhana@upnm.edu.my](mailto:norhana@upnm.edu.my)

the Earth. In addition to plants, cellulose can be also formed by fungi, green algae, and tunicates. The cellulose from plant fiber has particularly huge potential in many applications, from flexible food biodegradable packaging, structural, military, antimicrobial material to scaffolds for tissue regeneration [9–15]. Intriguingly, it is reported that some specific bacteria can synthesize cellulose called bacterial cellulose (BC). In order to remove the extractable fraction in cellulosic fiber, the pre-treatment associated with special solvent, chemicals and techniques is crucial. This method may cause slight damages onto the fiber structure of cellulosic surface. Considering this, BC has a lot to offer. In 1886, Brown published the first report on the production of BC by *Acetobacter xylinum* [16]. BC is also commonly referred to as “microbial cellulose” which is found as a gelatinous membrane at the liquid-air interface of the culture medium [17]. BC is produced at certain culture conditions by a number of bacteria belonging to the genera: *Achromobacter*, *Aerobacter*, *Agrobacterium*, *Alcaligenes*, *Azotobacter*, *Gluconacetobacter*, *Rhizobium*, and *Salmonella* [18]. The BC produced by *Acetobacter* strains bacteria, free from lignin, pectin, hemicellulose and other biogenetic products associated with plant cellulose, consists of metastable cellulose type I<sub>α</sub> (triclinic formation) with an exceptionally high purity of 70–90% and is characterized by 3D ultrafine fibril network structure, large surface area and aspect ratio, high porosity, high water absorption capacity (up to 400 times its dry weight), and high mechanical strength. The molecular configuration of constituted parallel arrangement of β(1→4)glycosidic chain, so called cellulose type I in BC, is insoluble in common organic solvents [19]. In terms of mechanical strength, the BC pellicles (membranes) containing 99% water show a tensile strength of 0.9 MPa, which dramatically increases to 240 MPa when the water content in the BC pellicles is reduced to 8% [20]. As a result, the higher cellulose content in BC potentially becomes a reinforcement for various applications like cellulose extracted from the plant fiber [21–23].

In this study, BC produced from fermentation of coconut water was called Nata de Coco. This BC was a white gelatinous cellulose produced from the fermentation of *Acetobacter aceti* *Xylinum* ssp. using fruit juice as a medium. Nata de Coco is one of the most famous desserts in Asian countries, including the Philippines, Indonesia, and Taiwan. It has high water content, which exceeds 90%, with low calorific value, and has high fiber content. It is a favorite delicacy to the native of the Philippines and is produced mainly from coconut water. Previous research reported that film produced by *Acetobacter aceti* subspecies *Xylinum* contained water and cellulose as the main component [24]. Besides, previous researches by Wei *et al.* [25] reported that the dried Nata de Coco was preferred rather than a wet form since it is more convenient and portable for practical application. Another study by Pa'e *et al.* [26] on different drying methods resulted in differ-

ent properties of Nata de Coco. Dried Nata de Coco produced by freeze drying showed the highest crystallinity (88.9%), swelling ability (490%), and tensile strength (148.01 MPa) compared with oven and tray dried. The dried Nata de Coco which possesses stable properties is suitable for powder processing.

Therefore, drying methods are crucial to structure, for performance and application of BC as reinforcement in polymer composites especially in automotive, aerospace, membrane filtration, and electronics applications [10, 27, 28]. Three different methods of production BC from Nata de Coco (*Acetobacter xylinum*), by drying, chemical and mechanical treatment, were investigated. The BC sheet was produced by drying in an oven until it reached a constant weight. The chemical treatment involved hydrolyzing by acid treatment diluted in 65% of sulphuric acid (H<sub>2</sub>SO<sub>4</sub>) to produce BC chem. The BC mech powder sample was produced by drying in the oven at 60°C, blending using a universal laboratory blender and finally was subjected to the grinding process. A series of analyses were performed to compare the properties of the product, including structural test XRD and FTIR and morphological test using FESEM.

## EXPERIMENTAL PART

### Materials

Nata de Coco (Figure 1) is a jelly-like food product produced by fermentation of coconut water using *Acetobacter xylinum* bacteria. It was supplied by a local manufacturer of food-grade Nata de Coco operating in Selangor, Malaysia. Sulphuric acid (H<sub>2</sub>SO<sub>4</sub>) that was used for chemical treatment for BC was purchased from Sigma Aldrich. For the control sample, microcrystalline cellulose (MCC) was purchased from Sigma Aldrich, while the pharmaceutical-grade cotton fabrics were purchased from the local pharmacy.



Fig. 1. Nata de Coco jelly

## Methods

### Bacterial cellulose preparation

The raw Nata de Coco was processed into the three different types of cellulose. They were the oven dried bacterial cellulose sheet (BC sheet), chemically treated powder form bacterial cellulose (BC chem), and mechanically treated powder bacterial cellulose (BC mech). Sample preparation started with the cleaning process of Nata de Coco, in which the raw sample was washed, soaked and rinsed using distilled water in order to remove any impurities in the samples. The washing and rinsing processes were repeated two times daily until the pH of rinsing water became neutral (pH 5 to 7). The cleaning process was then continued by soaking the Nata de Coco in distilled water for 24 hours. These processes were repeated for one to two weeks at room temperature in order to neutralize and stabilize the pristine Nata de Coco.

### Preparation of oven dried bacteria cellulose (BC sheet)

The BC sheet was obtained by means of drying technique in a conventional Memmert oven. Firstly, the rectangular sheet of Nata de Coco was cut into dimension of 300 × 150 mm which was an appropriate size to accommodate the oven cavity as shown in Figure 2a. The wet sample went then in the oven at 60°C through a slow drying process for 3 to 5 days. In order to avoid overheating on the sample, oven temperature and sample conditions were consistently monitored. During the drying process, the sample was weighed daily until its weight remained unchanged with density of 1.7 to 1.8 g/cm<sup>3</sup>. The consistent weight indicated that water was successfully removed from the BC sheet. Finally, the dried BC sheet, shown in Figure 2b, was sealed and zipped in a plastic bag before being kept in desiccator to avoid moisture absorption.

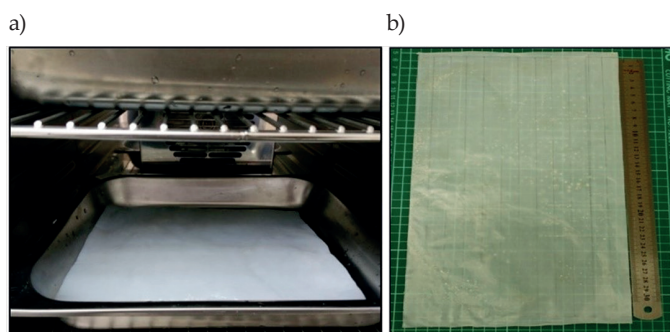


Fig. 2. Oven drying process (a), dried BC sheet sample (b)

### Preparation of chemically treated bacterial cellulose (BC chem)

BC chem powder was obtained via acid hydrolysis process. Before the chemical treatment took place, Nata de Coco cubes went through a drying process in the



Fig. 3. Centrifuge machine (a), supernatant precipitate (b), dried powder of chemically treated BC (c)

Memmert oven at 60°C for 24 hours. In a similar way as for BC sheet, the weight of Nata de Coco cube was monitored to ensure complete water removal from the samples. 10 g of dried BC cubes was then hydrolyzed by acid treatment using 65% H<sub>2</sub>SO<sub>4</sub> with diluted in 200 ml, at 45°C. The hydrolysis process took place under consistent stirring with a magnetic stirrer for about 45 minutes. The process produced a suspension that was filtered using a Buchner funnel under vacuum filtration. The collected liquid was then subjected to 5 times washing using centrifugation technique with the Eppendorf Germany centrifuge machine in (Figure 3a) at 10 000 rpm for 10 min. After each cycle of centrifugation, the collected white precipitate was diluted with 200 ml of cold deionized water before determining the pH value of the suspension. The washing process was considered adequate when the pH value reached 5 to 6. Precipitates from the final centrifugation cycle were then collected onto a Petri dish (Figure 3b) before it was left to dry



Fig. 4. Grinding of dried Nata de Coco powder (a), sieving of BC mech powder (b)

at ambient temperature for about 12 hours. Figure 3c shows the dried powder of BC chem, stored in a bottle to avoid moisture absorption before further analysis. The size of BC chem was in the range of 100  $\mu\text{m}$ .

#### Preparation of mechanically treated bacterial cellulose (BC mech)

White powder of BC mech was produced from the dried Nata de Coco cubes. In the same way as for the BC chem, the small size Nata de Coco was dried in the Memmert oven at 60°C for 3 to 5 days until the weight of dried cellulose remained unchanged. The dried BC was then blended using a laboratory universal blender (National MX 798S, Malaysia). After that blended BC was subjected to the manual grinding process (Figure 4a) by using mortar and sieved (Figure 4b) to produce finer BC mech powder. The size of BC mech was in the range of 125  $\mu\text{m}$ . Finally, the BC powder was kept in a bottle to prevent moisture absorbing.

#### X-ray diffraction (XRD) characterization

Crystallinity and crystallite size of the BC samples were studied by means of XRD technique. It was conducted using an X-ray diffractometer Siemens XRD D5000 equipped with copper anode Cu-K $\alpha$  ( $\lambda = 1.54 \text{ nm}$ ) radiation, operating at 40 kV/50 mA. The detector angle  $2\theta$  was set between 2° and 50° with a scan rate of 0.02°/min. XRD pattern was then analyzed using the Bragg's Law given in Eq. (1) [29]:

$$n\lambda = 2d \sin\theta \quad (1)$$

where:

$n$  – integer

$k$  – constant value ( $k = 0.89$ )

$\lambda$  – wavelength of the X-ray

$d$  – interplanar spacing generating the diffraction

$\theta$  – diffraction angle.

The peaks height calculations for the cellulose samples were determined using Expert Highscore software (Philips). The crystallinity index,  $XC$ , was calculated manually using Segal method [30]. The formula is shown as Eq. (2):

$$XC = (I_{002} - I_{am} / I_{002}) \cdot 100 \quad (2)$$

where:

$I_{002}$  – maximum intensity of diffraction peak from (002) lattice at an angle  $2\theta$  between 22° and 23°

$I_{am}$  – diffraction intensity of the amorphous phase taken at an angle  $2\theta$  between 15° to 19° with the intensity at minimum level [31].

The average crystallite size was calculated using Scherrer formula [32] on the diffraction peak from the (002) lattice plane as shown in Eq. (3):

$$D_{hkl} = k\lambda/\beta \cos\theta \quad (3)$$

where:

$D_{hkl}$  – crystallite dimension in perpendicular direction to the crystallographic plane ( $hkl$ )

$\theta$  – the Bragg angle

$\lambda$  – radiation wavelength

$\beta$  – full width high maximum (FWHM)

$k$  – Scherrer constant ( $k = 0.84$ ) [33].

#### Fourier transform infrared (FTIR) spectroscopy characterization

The vibrational structural characteristics analysis of chemical functional groups in the MCC, cotton fibers, and BC samples was done using FTIR. This technique also confirmed that BC produced from Nata de Coco was pure cellulose compared with cellulose produced from plant reported by the study on functional groups in the polymer cellulose molecules itself. Any elements that chemically took part in the sample chain could be detected. FTIR spectra of cellulosic samples were recorded in the transmittance range of 400  $\text{cm}^{-1}$  to 4000  $\text{cm}^{-1}$  with the resolution 4  $\text{cm}^{-1}$  using Perkin Elmer Spectrum 400 FTIR.

#### Field emission scanning electron microscopy (FESEM) characterization

The morphological analysis was conducted using FESEM in order to investigate the molecular surface structure or morphology of the structure. The samples were investigated using JEOL JSM-7600F FESEM. The morphology of various cellulose materials was characterized at an appropriate magnification. All samples were characterized at magnification of 1000 $\times$  and 2000 $\times$ , and further 5000 $\times$  only for BC sheet.

## RESULTS AND DISCUSSION

### XRD analysis

XRD patterns for BC sheet, BC chem, BC mech, MCC, and cotton fibers samples are shown in Figure 5 and Figure 6. Diffraction peaks in the diffractogram are attributed to crystalline scattering, while the diffuse background to amorphous region. According to International Centre for Diffraction Data® (ICDD®), diffraction peaks of native cellulose are located around  $2\theta = 14.90^\circ$ ,  $16.49^\circ$ , and  $22.84^\circ$ , which correspond respectively to the (001), (110), and (002) crystal lattices. In Figure 5, XRD peaks from BC sheet are located at  $2\theta = 14.15^\circ$ ,  $16.25^\circ$ , and  $22.46^\circ$ , while MCC at  $2\theta = 14.72^\circ$ ,  $16.33^\circ$ , and  $22.79^\circ$ , and cotton fiber at  $2\theta = 14.46^\circ$ ,  $16.80^\circ$ , and  $22.85^\circ$ , respectively. These peaks demonstrate a typical set of diffraction peaks for cellulose I. Oudiani *et al.* [31] and Klemm *et al.* [34] reported similar peaks in their work on cellulose. It is proven that BC sheet is a native cellulose or cellulose I (Figure 5). Further anal-

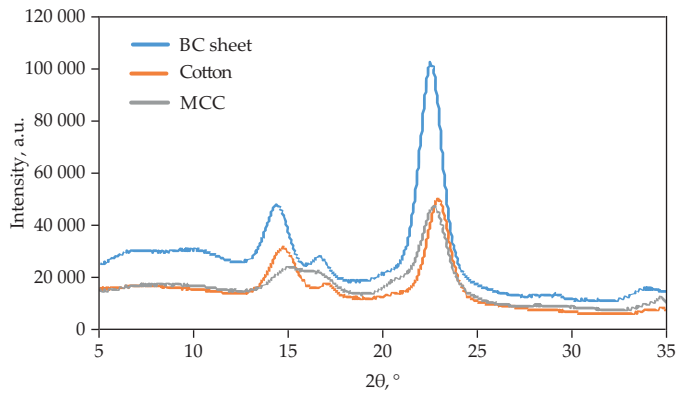


Fig. 5. XRD patterns of BC sheet, cotton fiber, and MCC

ysis showed that cotton peaks resembled those of ICDD, especially diffraction peaks from the (002) lattice plane where  $2\theta_{\text{cotton}} = 22.85^\circ$  and  $2\theta_{\text{ICDD}} = 22.84^\circ$ . These values were in agreement since the ICDD data represent  $I_\beta$  polymorph, which is known as dominant in plant-based cellulose. Similar peak from BC sheet at  $2\theta = 22.46^\circ$  on the other hand shows significant difference of about  $0.38^\circ$ . This peak indicated the presence of  $I_\beta$  polymorph that is prevalent in BC [35, 36]. It means that XRD peaks  $14.15^\circ$ ,  $16.25^\circ$ , and  $22.46^\circ$  of BC sheet demonstrated diffraction patterns from (001), (110), and (200) crystal lattices, in that order.

Despite the chemical and mechanical treatment, (001), (110), and (200) crystal lattices in both BC chem and BC mech samples managed to produce peaks around  $14^\circ$  to  $23^\circ$  similarly to the BC sheet. However, Figure 6 shows that diffraction peaks in BC chem and BC mech became relatively smaller as compared to those of BC sheet. From Table 1, the BC sheet peaks were shifted to  $2\theta = 14.38^\circ$ ,  $16.80^\circ$ , and  $22.74^\circ$  in case of BC chem and  $2\theta = 14.17^\circ$ ,  $16.48^\circ$ , and  $22.63^\circ$  in case of BC mech. It means that modification by means of mechanical and chemical treatment caused some changes in interplanar distance. For example, the basal distance spacing  $d = 3.96 \text{ \AA}$  of (200) lattice plane in BC sheet was reduced to  $d = 3.93 \text{ \AA}$  (BC mech)

Table 1. XRD peaks for BC sheet, BC mech, and BC chem

Lattice plane, $hkl$	$2\theta_{001}$ , °	$2\theta_{110}$ , °	$2\theta_{002}$ , °	Type of cellulose
ICDD Standard value of cellulose $I_\beta$	14.90	16.49	22.84	$I_\beta$
BC sheet	14.15	16.25	22.46	$I_a$
BC chem	14.38	16.80	22.74	$I_a$
BC mech	14.17	16.48	22.63	$I_a$
MCC	14.72	16.33	22.79	$I_\beta$
Cotton	14.46	16.80	22.85	$I_\beta$
ICDD Standard value of cellulose II	12.10	19.80	22.00	II

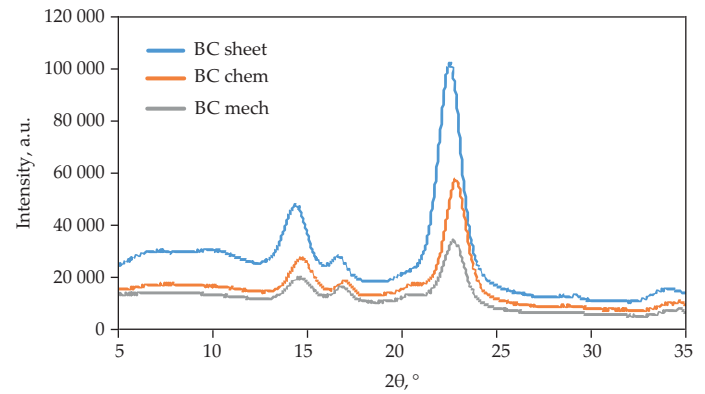


Fig. 6. XRD patterns of BC sheet, BC chem, and BC mech

and  $3.91 \text{ \AA}$  (BC chem). The peaks summarized in Table 1 show that the BC products lie in the type of cellulose I which is a native cellulose. All celluloses exist in both  $I_\alpha$  (typical bacterial and algal cellulose) and  $I_\beta$  (typical plant and wood cellulose).

#### Crystallinity and crystallite size

Crystallinity of cellulose is defined as the weight fraction of the crystalline phase known as crystalline cellulose. The basal distance spacing  $d$ , full width high maximum (FWHM), crystallinity indices ( $X_{002}$ ), and crystallite sizes of cellulose samples are given in Table 2. Diffraction peak from (200) plane was used in the calculation of  $XC$  and  $D_{002}$  since it is a prominent crystallite peak in cellulose [37]. Basing on Table 2,  $XC$  and  $D_{002}$  of BC sheet were  $81.76\%$  and  $4.55 \text{ nm}$ , respectively, whereas for cotton  $XC = 75.73\%$  and  $D_{002} = 6.83 \text{ nm}$ . This was due to different types of dominant polymorphs in both celluloses:  $I_\beta$  is prevalent in cotton and BC sheet is dominated by the  $I_\alpha$  polymorph. Crystallinity index and crystallite size in comparison with cotton and MCC decreased and for MCC they were  $XC = 72.06\%$  and  $D_{002} = 4.97 \text{ nm}$ . Chemical and mechanical processes on plant-based cellulose in order to produce the MCC should change the crystallite properties. In the same way, chemical and mechanical treatment on pristine BC caused a reduction in crystallinity index  $XC = 81.76\%$  (BC sheet) to  $76.13\%$  (BC chem) and  $67.27\%$  (BC mech). Several researchers reported the decrease in

Table 2. Basal distance spacing  $d$ , FWHM, crystallinity indices ( $X_{002}$ ), and crystallite sizes of BC sheet, BC chem, and BC mech

Sample	$2\theta_{002}$ , °	$d_{002}$ , Å	FWHM	$D_{002}$ , nm	$X_{002}$ , %
BC sheet	22.46	3.9608	0.3070	4.55	81.76
BC chem	22.74	3.9103	0.2047	6.83	76.13
BC mech	22.63	3.9299	0.1535	9.11	67.27
MCC	22.79	3.9013	0.2814	4.97	72.06
Cotton	22.85	3.8911	0.2047	6.83	75.73

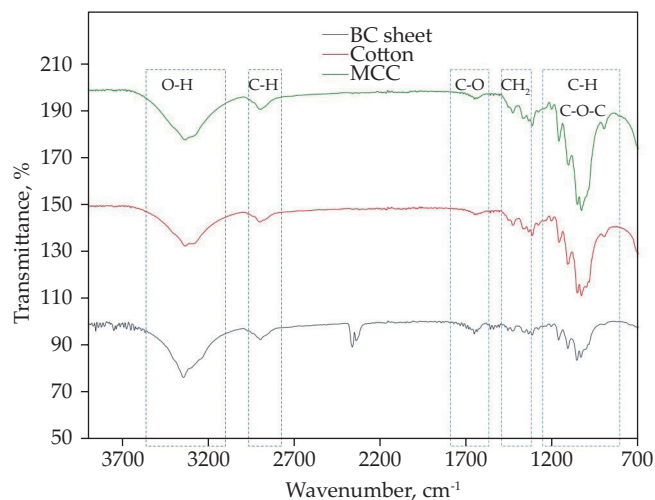


Fig. 7. FTIR spectra for BC sheet, cotton, and MCC

crystallinity after the acid treatment due to the process of obtaining cellulose itself [38]. In this work, however, acid hydrolysis reduced the crystallinity index of BC. It was able to increase the amorphous phase better than the mechanical process in BC mech. On the other hand, the crystallite size was improved due to the chemical and mechanical processes. A significant increase in crystallite size could be seen from  $D_{002} = 4.55$  nm in BC sheet to  $D_{002} = 6.83$  nm and 9.11 nm in BC chem and BC mech, respectively.

### FTIR analysis

The main structure of cellulose is carbon, hydrogen, and oxygen group  $[(C_6H_{10}O_5)_n]$ . Figure 7 displays the FTIR spectra for BC sheet, cotton, and MCC. The aim of this analysis of BC sheet, cotton fabrics, and commercial MCC is to compare the existing of main functional groups of cellulose in the prepared BC samples. For the BC sheet spectrum, distinguished peaks of  $3330\text{ cm}^{-1}$  indicated O-H stretching,  $2880\text{ cm}^{-1}$  and  $1310\text{ cm}^{-1}$  indicated aliphatic C-H stretching vibration,  $1630\text{ cm}^{-1}$  and  $1050\text{ cm}^{-1}$  indicated C-O stretching,  $1420\text{ cm}^{-1}$  indicated  $\text{CH}_2$  bending, and  $1160\text{ cm}^{-1}$  indicated a sharp and steep band to the presence of C-O-C stretching vibrations. The O-H and C-H bonds of MCC and cotton existed in spectrum of  $3320\text{ cm}^{-1}$  and  $2890\text{ cm}^{-1}$  [39]. Both MCC and cotton fabrics had the same spectra number at  $1420\text{ cm}^{-1}$ ,  $1310\text{ cm}^{-1}$ , and  $1100\text{ cm}^{-1}$ , which indicated  $\text{CH}_2$ , C-H, and C-O-C accordingly. The O-H stretching of MCC and cotton differed about  $10\text{ cm}^{-1}$  in the spectral range comparing with BC sheet. They lie at the same spectra of  $\text{CH}_2$ , C-H, and C-O-C as described in Figure 7. All the spectra seem to differ only about  $10$  to  $20\text{ cm}^{-1}$  in case of BC sheet, MCC, and cotton. Thus, the spectra of BC sheet, MCC, and cotton shown in Figure 7 confirmed that cellulose produced by bacteria was pure and comparable with cellulose from the commercial one. These spectra also followed the spectrum of hardwood which shows strong

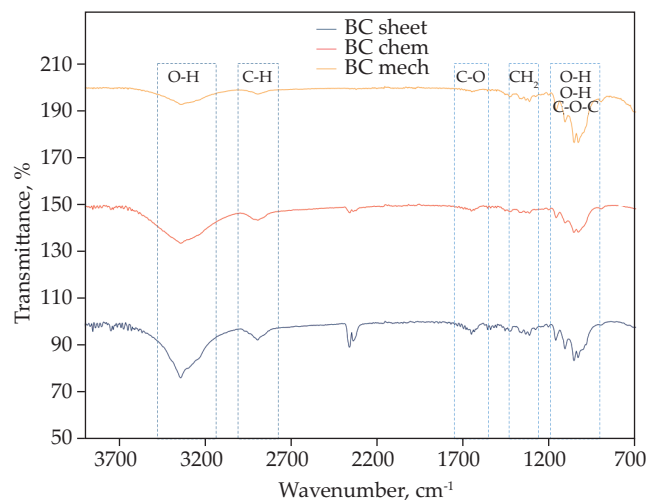


Fig. 8. FTIR spectra of BC sheet, BC chem, and BC mech

broad O-H stretching ( $3300$  to  $4000\text{ cm}^{-1}$ ), C-H stretching in methyl and methylene groups ( $2800$  to  $3000\text{ cm}^{-1}$ ), and a strong broad superposition with sharp and discrete absorptions in the region from  $1000$  to  $1750\text{ cm}^{-1}$  [40].

Figure 8 presents the FTIR spectra for BC sheet, BC chem and BC mech powders. All the values detected in the both functional group spectra in Figure 7 and Figure 8 are given in the Table 3. The functional groups of prepared BC seem to have almost near number of values with each other and with the commercial one. All the cellulose samples contained strong broad hydroxyl group (O-H) at IR spectra of  $3200$  to  $3400\text{ cm}^{-1}$  and sharp band around  $1170$  to  $1150\text{ cm}^{-1}$ . Previous study of hydrogen bonding in native cellulose demonstrated that inter-chain hydrogen bonds which keep cellulose chains aligned in sheets, resulted in high degree of crystallinity of cellulose [41]. From Figure 8, the intensity of O-H bands around  $1310\text{ cm}^{-1}$  decreased after chemical and mechanical treatments of the BC structure due to reduction of crystallinity in BC chem and BC mech. Similar trend could be seen on the O-H band around  $3330\text{ cm}^{-1}$  of BC mech but not in the spectra of BC chem. The O-H band intensity seemed to increase indicating the effect of water, which was the reaction medium used during chemical treatment. Vibrational band for methylene group which appeared within  $2800$  and  $3000\text{ cm}^{-1}$  indicated the C-H stretching mode. C-H and  $\text{CH}_2$  bending bands also confirmed the functional groups of cellulose which can be observed around  $1400$  to  $1350\text{ cm}^{-1}$  and are given accordingly in Table 3. Although fingerprints bands can confirm the structure of prepared BC, the peaks may vary depending on the origin of cellulose. All the peaks correspond to cellulose but the shape of curve may differ from each other. The FTIR analysis confirmed that BC is as pure with the existed cellulose.

### FESEM analysis

The comparison of morphological properties through FESEM of BC sheet, BC chem, BC mech, MCC, and cotton

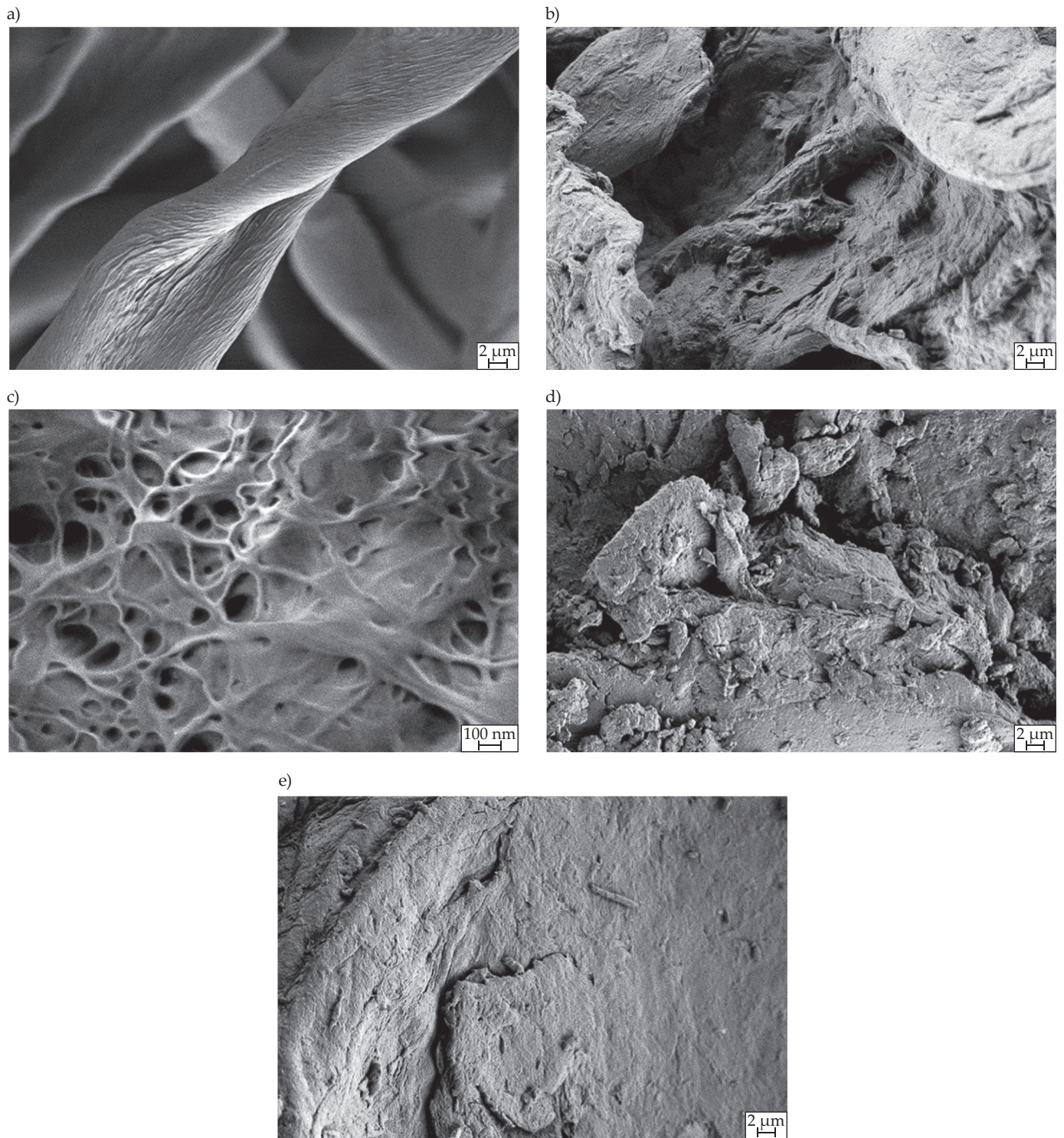


Fig. 9. FESEM images: a) of cotton fabric, b) MCC, c) BC sheet, d) BC chem, e) BC mech

is presented in Figure 9. BC sheet under 2000 $\times$  magnification in Figure 9c looks like a piece of close-woven fibrous cloth but similar magnification on cotton fiber in Figure 9a demonstrates strands of cellulose ribbon with an average diameter of 16  $\mu\text{m}$ . Further magnification of 5000 $\times$  in Figure 9c on the BC sheet shows an aggregated web-like structure, comprising interlocking yarn with intertwined nano-threads known as nanofibrils. BC chem and MCC show an average size of 20 to 40  $\mu\text{m}$ , while BC mech has

a larger size than then with an average of 30 to 60  $\mu\text{m}$ . From Figure 9d and Figure 9e, the cellulose structure of BC chem and BC mech seems to agglomerate, as well as in MCC (Figure 9b). This might be due to the structure of the powder of BC chem, and BC mech might have changed due to the treatment of the sample preparation itself [45]. The observations explain the increased crystallite structure of BC chem and BC mech noticed in XRD results, and in-lines with the FTIR results, where chemical treat-

**Table 3.** Functional group analysis of BC sheet, BC chem, and BC mech

Wavenumber, cm <sup>-1</sup>					Functional group	Ref.
BC sheet	BC chem	BC mech	MCC (control sample)	Cotton fabrics (control sample)		
3330	3328	3330	3320	3320	O-H stretching	[32, 42–44]
2880	2882	2870	2890	2890	C-H stretching	
1630	1634	1640	1640	1630	C-O bonds	
1420	1416	1420	1420	1420	CH <sub>2</sub> bending	
1310	1309	1310	1310	1310	C-H bending	
1160	1154	1160	1160	1150	C-O-C stretching	
1100	1101	1110	1100	1100	C-O-C stretching	
1050	1051	1050	1030	1050	C-O stretching	
891	889	894	892	890	CH <sub>2</sub> bending	

ment of these samples removed the hydrocarbon chain in BC and increased the OH group's presence. However, the OH groups facilitate the interaction among particles through hydrogen bonding, leading to agglomeration. Long, smooth and oriented fibrils bundle of width within range 30 to 100 nm of BC sheet, 20 to 60 μm for the BC chem and BC mech powder cellulose is observed.

### CONCLUSIONS

In conclusion, the pre-treatment for BC from *Nata de Coco* (*Acetobacter xylinum*) has been successfully done through oven drying, chemical treatment, and mechanical treatment. The crystallinity index had the highest value for a sample of BC sheet with 81.76% in comparison with cotton fabrics from cellulose (75.73%). Acid hydrolysis reduced the crystallinity index of BC. It was able to increase the amorphous phase better than the mechanical process in BC mech. On the other hand, the crystallite size was improved due to the chemical and mechanical processes with a significant increase in crystallite size from  $D_{002} = 4.55$  nm in BC sheet to  $D_{002} = 6.83$  nm and 9.11 nm in case of BC chem and BC mech, respectively. The FTIR results confirmed that these samples are BC with the presence of bands appearing at 3330 cm<sup>-1</sup> (O-H), 2880 cm<sup>-1</sup> (C-H), 1310 cm<sup>-1</sup> (C-H), 1420 cm<sup>-1</sup> (CH<sub>2</sub>), 1160 cm<sup>-1</sup> (C-O-C), and 1050 cm<sup>-1</sup> (C-O) stretching. In a picture of the morphology structure of the BC sheet, the fiber seems to have better arrangement than agglomerations that occurred in BC chem and BC mech surface morphological analysis. BC sheet was identified as the best candidate for further composite fabrication because of its the highest crystallinity percentage and strong hydrogen bonding observed, and web-like structures of nanofibrils that offer huge contact surface for interphase interaction able to provide high surface area and contact with the matrix.

### ACKNOWLEDGEMENTS

The authors would like to acknowledge the financial support from The Ministry of Higher Education under the Niche

Research Grant Scheme (NRGS) NRGS/2013/UPNM/PK/P1 and Universiti Pertahanan Nasional Malaysia (UPNM) for the technical supports.

### REFERENCES

- [1] Soatthiyanon N., Aumnate C., Srikulkit K.: *Polymer Composites* **2020**, *41*, 2777.  
<https://doi.org/10.1002/pc.25575>
- [2] Asyraf M.R.M., Rafidah M., Azrina A. et al.: *Cellulose* **2021**, *28*, 2675.  
<https://doi.org/10.1007/s10570-021-03710-3>
- [3] Ilyas R.A., Sapuan S.M., Atikah M.S.N. et al.: *Textile Research Journal* **2021**, *91*, 152.  
<https://doi.org/10.1177/0040517520932393>
- [4] Ilyas R.A., Sapuan S.M., Atiqah A. et al.: *Polymer Composites* **2020**, *41*, 459.  
<https://doi.org/10.1002/pc.25379>
- [5] Wijaya C.J., Ismadji S., Aparamarta H.W. et al.: *ACS Omega* **2020**, *5*, 20967.  
<https://doi.org/10.1021/acsomega.0c02425>
- [6] He B., Wang W., Song Y. et al.: *International Journal of Biological Macromolecules* **2020**, *164*, 1649.  
<https://doi.org/10.1016/j.ijbiomac.2020.07.286>
- [7] Lai D.S., Osman A.F., Adnan S.A. et al.: *Polymers* **2021**, *13*, 897.  
<https://doi.org/10.3390/polym13060897>
- [8] Ismail F., Othman N.E.A., Wahab N.A. et al.: *Journal of Oil Palm Research* **2020**, *32*, 621.  
<https://doi.org/10.21894/jopr.2020.0057>
- [9] Sharip N.S. et al.: "A review on nanocellulose composites in biomedical application", Chapter 8, "Composites in Biomedical Applications" CRC Press, 2020, pp. 161–190.
- [10] Norrrahim M.N.F., Nurazzi N.M., Jenol M.A. et al.: *Materials Advances* **2021**, *2*, 3538.  
<https://doi.org/10.1039/D1MA00116G>
- [11] Norrrahim M.N.F., Sapuan M.S., Ilyas R.A.: "Performance evaluation of cellulose nanofiber reinforced polypropylene biocomposites for automotive applications", Chapter 7, "Biocomposite and Synthetic Composites for Automotive Applications" Elsevier, 2021, pp. 199–215.

- <https://doi.org/10.1016/B978-0-12-820559-4.00007-9>
- [12] Asyraf M.R.M., Ishak M.R., Norrrahim M.N.F. *et al.*: *International Journal of Biological Macromolecules* **2021**, 193B, 1587.  
<https://doi.org/10.1016/j.ijbiomac.2021.10.221>
- [13] Norrrahim M.N.F., Ilyas R.A., Nurazzi N.M. *et al.*: *Applied Science and Engineering Progress* **2021**, 14, 588.  
<https://doi.org/10.14416/j.asep.2021.07.004>
- [14] Ilyas R.A., Azmi A., Nurazzi N.M. *et al.*: *materialstoday: Proceedings* **2022**, 52, 2414.  
<https://doi.org/10.1016/j.matpr.2021.10.420>
- [15] Norrrahim M.N.F. *et al.*: “Biocompatibility, Biodegradability, and Environmental Safety of PLA/Cellulose Composites”, Chapter 12, “Polylactic Acid-Based Nanocellulose and Cellulose Composites” CRC Press, 2022, pp. 251–264.
- [16] Brown A.J.: *Journal of the Chemical Society, Transactions* **1886**, 49, 432.  
<https://doi.org/10.1039/CT8864900432>
- [17] Kamide K., Matsuda Y., Iijima H. *et al.*: *British Polymer Journal* **1990**, 22, 167.  
<https://doi.org/10.1002/pi.4980220212>
- [18] Rangaswamy B.E., Vanitha K.P., Hungund B.S.: *International Journal of Polymer Science* **2015**, 2015, ID: 280784.  
<https://doi.org/10.1155/2015/280784>
- [19] Abbott A.: “Bacterial cellulose for use in hierarchical composites, macroporous foams, bioinorganic nanohybrids and bacterial-based nanocomposites” Ph.D. Diss., Imperial College London, 2011.  
<https://doi.org/10.25560/8976>
- [20] Scionti G.: “Mechanical properties of bacterial cellulose implants” M.Sc. Thesis, Chalmers University of Technology, 2010.
- [21] Nurazzi N.M., Asyraf M.R.M., Athiyah S.F. *et al.*: *Polymers* **2021**, 13, 2170.  
<https://doi.org/10.3390/polym13132170>
- [22] Nurazzi N.M., Khalina A., Sapuan S.M. *et al.*: *Journal of Mechanical Engineering and Sciences* **2017**, 11, 2650.  
<https://doi.org/10.15282/jmes.11.2.2017.8.0242>
- [23] Ilyas R.A., Sapuan S.M., Norizan M.N. *et al.*: “Potential of natural fibre composites for transport industry: A review” in “Prosiding Seminar Enau Kebangsaan” Persatuan Pembangunan dan Industri Enau Malaysia (PPIEM) Bahau, 2019, pp. 2–11.
- [24] Mohammad S.M., Rahman N.A., Khalil M.S. *et al.*: *Advances in Biological Research* **2014**, 8(6), 307.  
<https://doi.org/10.5829/idosi.abr.2014.8.6.1215>
- [25] Wei B., Yang G., Hong F.: *Carbohydrate Polymers* **2011**, 84, 533.  
<https://doi.org/10.1016/j.carbpol.2010.12.017>
- [26] Pa'e N., Hamid N.I.A., Khairuddin N. *et al.*: *Sains Malaysiana* **2014**, 43(5), 767.
- [27] Norrrahim M.N.F., Kasim N.A.M., Knight V.F. *et al.*: *Functional Composites and Structures* **2021**, 3, 024001.  
<https://doi.org/10.1088/2631-6331/abeef6>
- [28] Norrrahim M.N.F., Yasim-Anuar T.A.T., Jenol M.A. *et al.*: “Performance evaluation of cellulose nanofiber reinforced polypropylene biocomposites for automotive applications”, Chapter 7, “Biocomposite and synthetic composites for automotive applications” Woodhead Publishing Series, Amsterdam, The Netherlands, 2020.  
<https://doi.org/10.1016/B978-0-12-820559-4.00007-9>
- [29] Yu H., Qin Z., Liang B. *et al.*: *Journal of Materials Chemistry A* **2013**, 1, 3938.  
<https://doi.org/10.1039/C3TA01150J>
- [30] Segal L., Creely J.J., Martin A.E. *et al.*: *Textile Research Journal* **1959**, 29, 786.  
<https://doi.org/10.1177/004051755902901003>
- [31] El Oudiani A., Chaabouni Y., Msahli S. *et al.*: *Carbohydrate Polymers* **2011**, 86, 1221.  
<https://doi.org/10.1016/j.carbpol.2011.06.037>
- [32] Zeng M., Laromaine A., Roig A.: *Cellulose* **2014**, 21, 4455.  
<https://doi.org/10.1007/s10570-014-0408-y>
- [33] Mohkami M., Talaeipour M.: *Bioresources* **2011**, 6, 1988.
- [34] Klemm D., Kramer F., Moritz S. *et al.*: *Angewandte Chemie International Edition* **2011**, 50, 5438.  
<https://doi.org/10.1002/anie.201001273>
- [35] Keshk S.M.: *Journal of Bioprocessing & Biotechniques* **2014**, 4, 2.  
<https://doi.org/10.4172/2155-9821.1000150>
- [36] Ilyas R.A., Sapuan S.M., Ibrahim R. *et al.*: *Journal of Materials Research and Technology* **2019**, 8, 4819.  
<https://doi.org/10.1016/j.jmrt.2019.08.028>
- [37] Park S., Baker J.O., Himmel M.E. *et al.*: *Biotechnology for Biofuels and Bioproducts* **2010**, 3, ID: 10.  
<https://doi.org/10.1186/1754-6834-3-10>
- [38] Samzadeh-Kermani A., Esfandiary N.: *Advances in Nanoparticles* **2016**, 5, 18.  
<https://doi.org/10.4236/anp.2016.51003>
- [39] Ilyas R.A., Sapuan S.M., Ibrahim R. *et al.*: *Journal of Materials Research and Technology* **2019**, 8, 2753.  
<https://doi.org/10.1016/j.jmrt.2019.04.011>
- [40] Bodîrlău R., Teacă C.A.: *Romanian Journal of Physics* **2009**, 54, 93.
- [41] Ansell M.P., Mwaikambo L.Y.: “The structure of cotton and other plant fibres”, Chapter 2, “Handbook of textile fibre structure” Elsevier, 2009, pp. 62–94.  
<https://doi.org/10.1533/9781845697310.1.62>
- [42] Rezanezhad S., Nazanezhad N., Asadpur G.: *Lignocellulose* **2013**, 2, 282.
- [43] Barud H.S., Ribeiro C.A., Crespi M.S. *et al.*: *Journal of Thermal Analysis and Calorimetry* **2007**, 87, 815.  
<https://doi.org/10.1007/s10973-006-8170-5>
- [44] Pandey M., Abeer M.M., Amin M.C.I.M.: *International Journal of Pharmacy and Pharmaceutical Sciences* **2014**, 6(6), 89.
- [45] Lu T., Jiang M., Jiang Z. *et al.*: *Composites Part B: Engineering* **2013**, 51, 28.  
<https://doi.org/10.1016/j.compositesb.2013.02.031>

Received 28 XII 2021.